Supplemental Figure 1

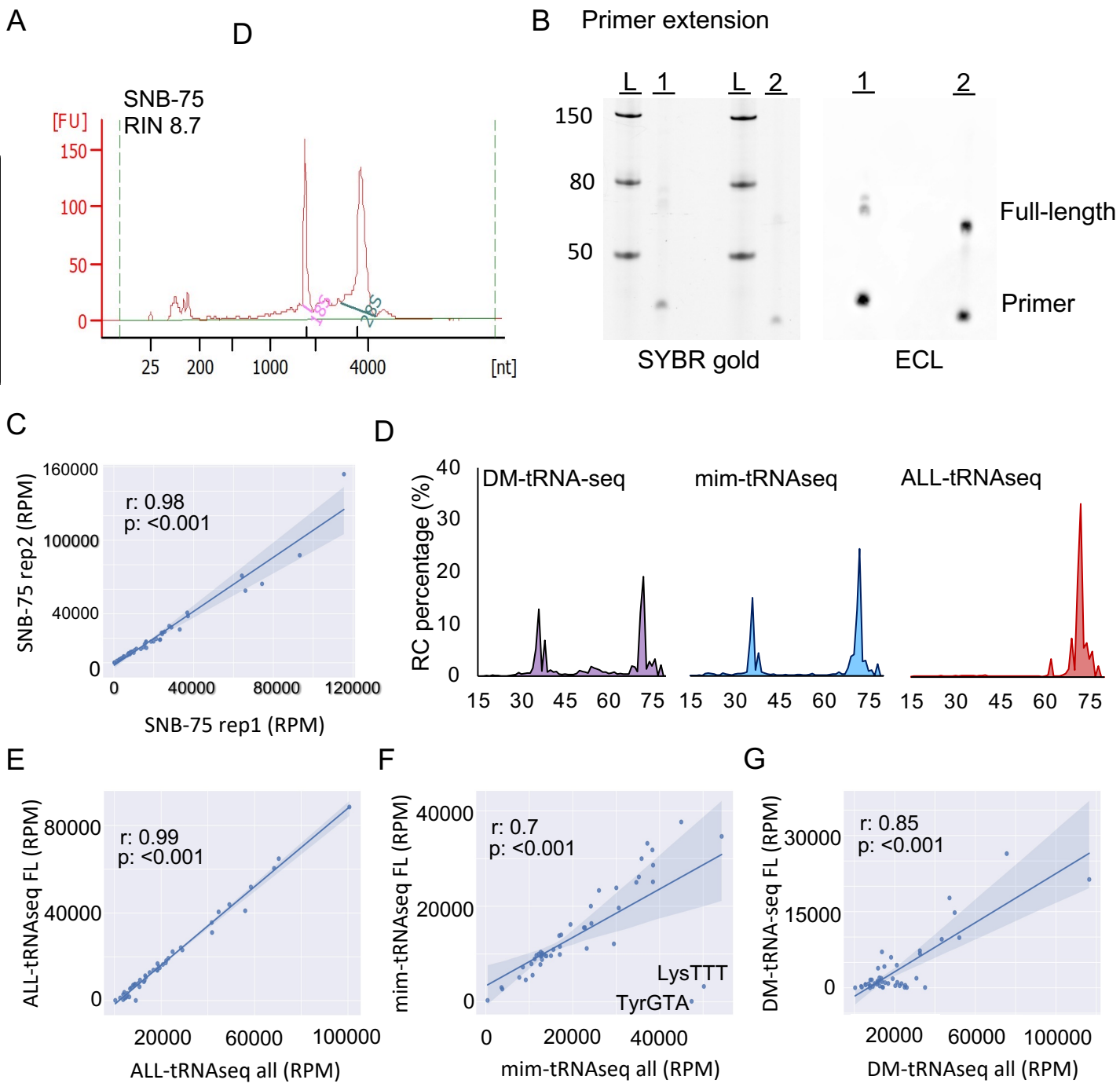

Figure S1. (A) Total RNA quality analysis showing electropherogram of SNB-75 sample using Bioanalyzer RNA 6000 Nano chip. (B) Primer extension analysis in tRNA-GlyGCC and tRNA-LysCTT using 2 ug demethylated total RNA from HEK293T cells. Left panels, SYBR gold staining of cDNA yields for tRNA-GlyGCC (1) and tRNA-LysCTT (2), and small RNA ladder (L; 50 nt, 80 nt and 150 nt) separated on a 10% denaturing polyacrylamide gel. Right panels, chemiluminescent detection of biotin-labeled cDNA products of tRNA-GlyGCC (left) and tRNA-LysCTT (right). (C) Pearson correlation (*r*: 0.98) between two technical replicates SNB-75 samples used in ALL-tRNAseq library preparation. (D) mt-tRNA read length distribution comparison between DM-tRNA-seq, mim-tRNAseq and ALL-tRNAseq, showed as percentage of all reads mapping to mitochondrial tRNA from HEK293T cells. (E) Pearson correlation (*r*: 0.99) between normalized full-length tRNA reads and all tRNA reads for each tRNA isodecoder detected in HEK293T by ALL-tRNAseq. (F) Pearson correlation (*r*: 0.7) between normalized full-length tRNA reads and all tRNA reads for each tRNA isodecoder using mim-tRNAseq library preparation of HEK293T RNA. The position of two outliers, tRNA-TyrGTA and tRNA-LysTTT, are indicated. (G) Pearson correlation (*r*: -0.85) between normalized full-length tRNA reads and all tRNA reads for each tRNA anticodon family detected in HEK293T by DM-tRNA-seq.

Supplemental Figure 2

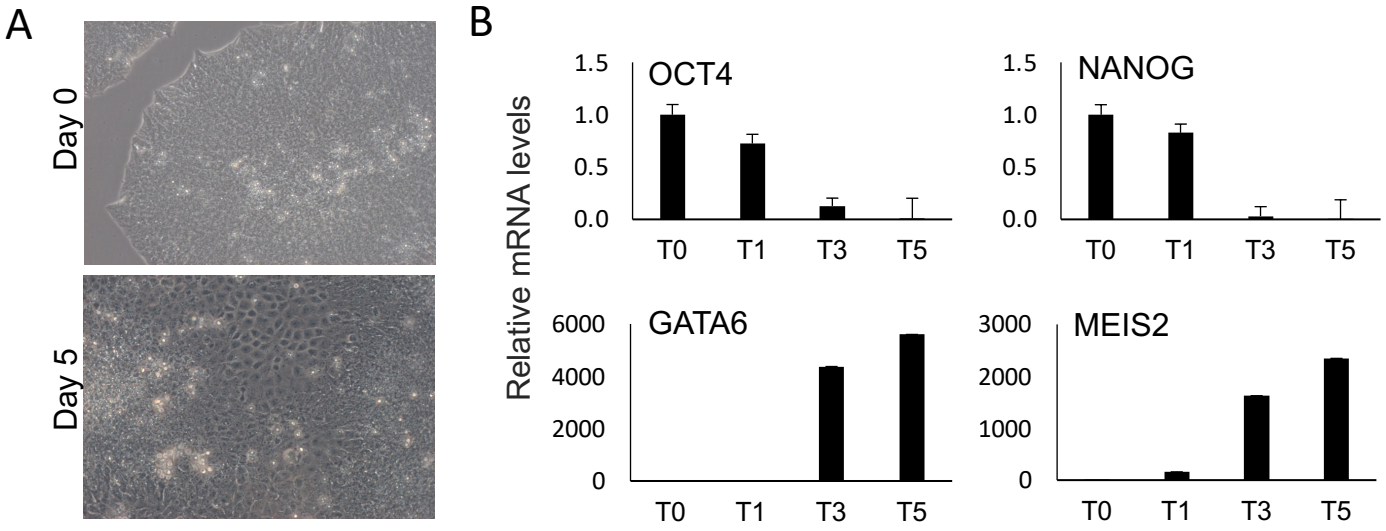

Figure S2. (A) Representative bright-field images of hESC colonies at day 0 and day 5 after ATRA-induced differentiation. (B) Relative mRNA levels of differentiation markers were measured using qRT-PCR in hESCs before and after ATRA-induced differentiation. Data are shown as mean ± SD of three replicates, data was normalized to GAPDH.

Supplemental Figure 3

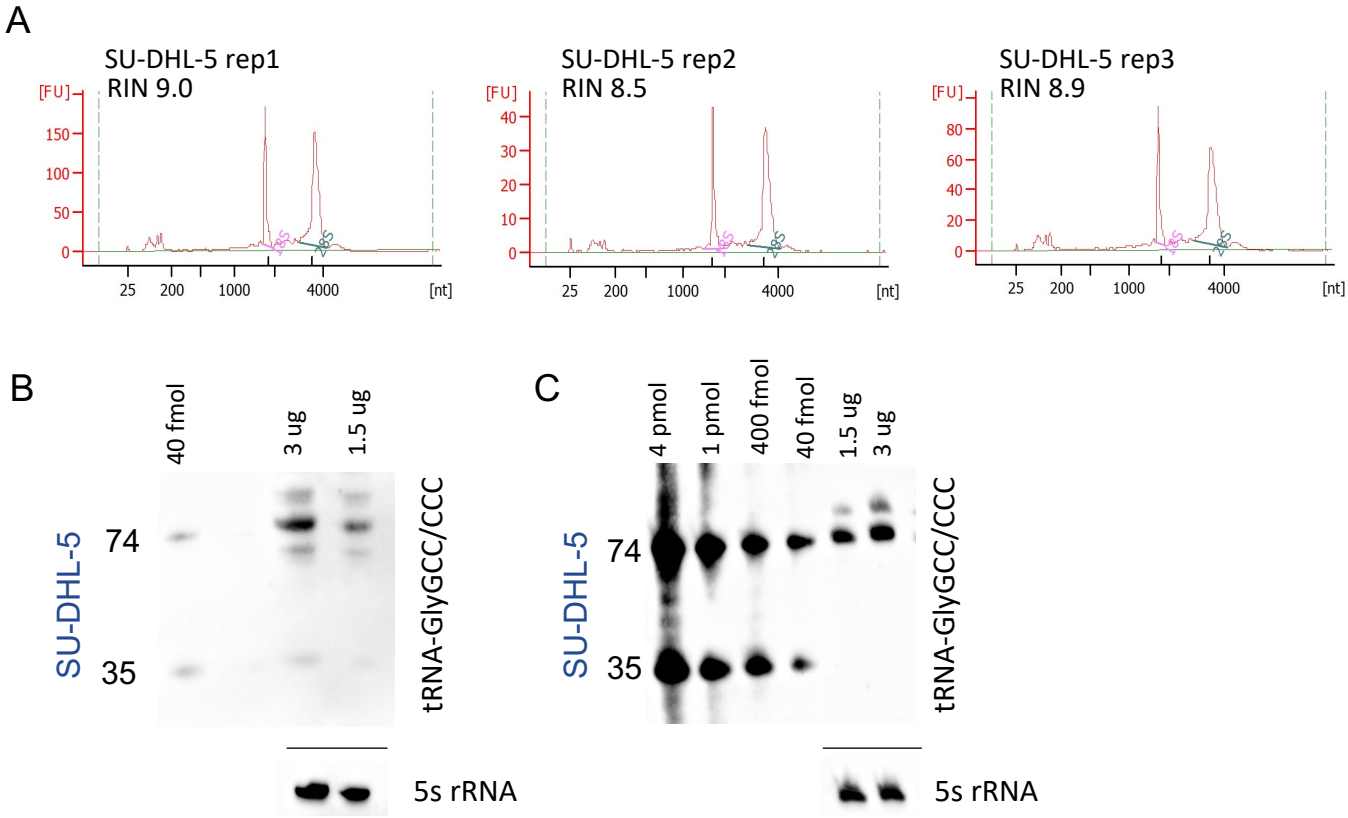

Figure S3. (A) Bioanalyzer electropherograms of three SU-DHL-5 replicates used in this study. (B) Validation of ALL-tRNAseq results in cell line SU-DHL-5 replicate 1 with northern blot examination of tRNA GlyGCC/CCC in synthetic tRNA GlyGCC oligonucleotides of 35nt and 74nt (left) and cell line SU-DHL-5 (right). 5s rRNA was used as a loading control. (C) Northern blot results of tRNA GlyGCC/CCC in synthetic tRNA GlyGCC oligonucleotides of 35nt and 74nt (left) and cell line SU-DHL-5. 5s rRNA was used as a loading control.

Supplemental Figure 4

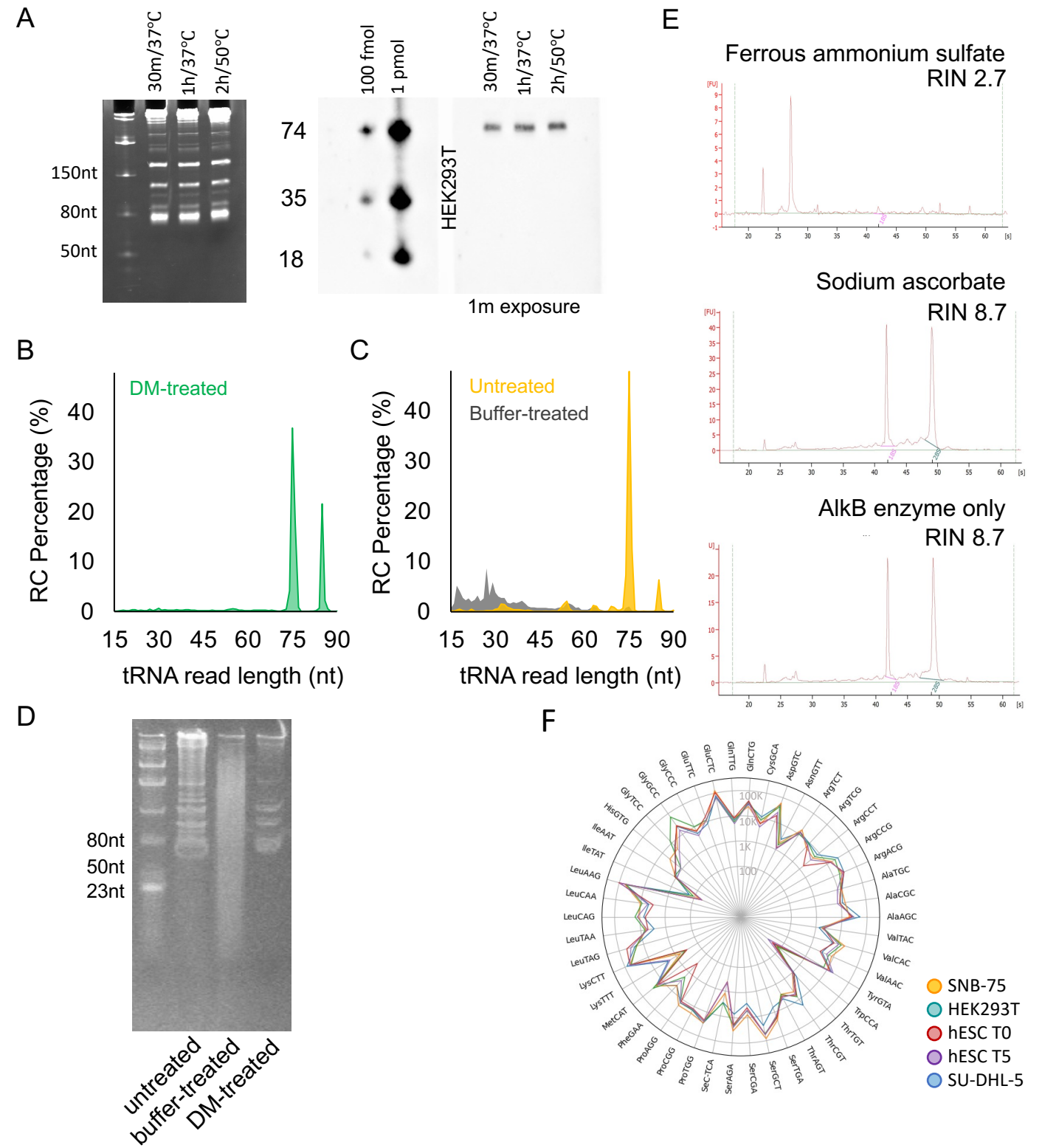

Figure S4. (A) Left panel, SYBR gold staining of HEK293T-extracted total RNAs subjected to deacylation treatment using Tris/EDTA (TE) and small RNA ladder (50 nt, 80 nt and 150 nt) separated on a 10% denaturing polyacrylamide gel. Middle and right panels, Northern blot detection of tRNA GlyGCC/CCC in synthetic tRNA GlyGCC oligonucleotides of 18nt, 35nt and 74nt (middle) and TE-treated HEK293T samples (right). (B) TRNA read length distribution in percentage with ALL-tRNAseq using MarathonRT for reverse transcription of DM-treated RNA total RNA from SNB-75 cells. (C) Comparison of tRNA read length distribution in percentage detected by ALL-tRNAseq using MarathonRT for reverse transcription of either untreated or buffer-treated RNA into cDNA in SNB-75 cell line. (D) SYBR gold staining of untreated total RNA, buffer-treated and DM-treated total RNA isolated from SNB-75 and low range ssRNA ladder in combination with FAM-labeled markers (23 nt and 39 nt) separated on a 10% denaturing polyacrylamide gel. (E) Bioanalyzer traces of total RNA incubated with ferrous ammonium sulfate (top), sodium ascorbate (middle) or AlkB enzyme only (bottom). (F) Radar plot of tRNA anticodon reads per million showing the distribution of full-length tRNA reads per tRNA anticodon for SNB-75 (orange line), HEK293T (green line), hESC T0 (red line), hESC T5 (purple line) and SNB-75 (blue line). Data are represented as Log 10 RPM values on the radius.

Supplemental Figure 5

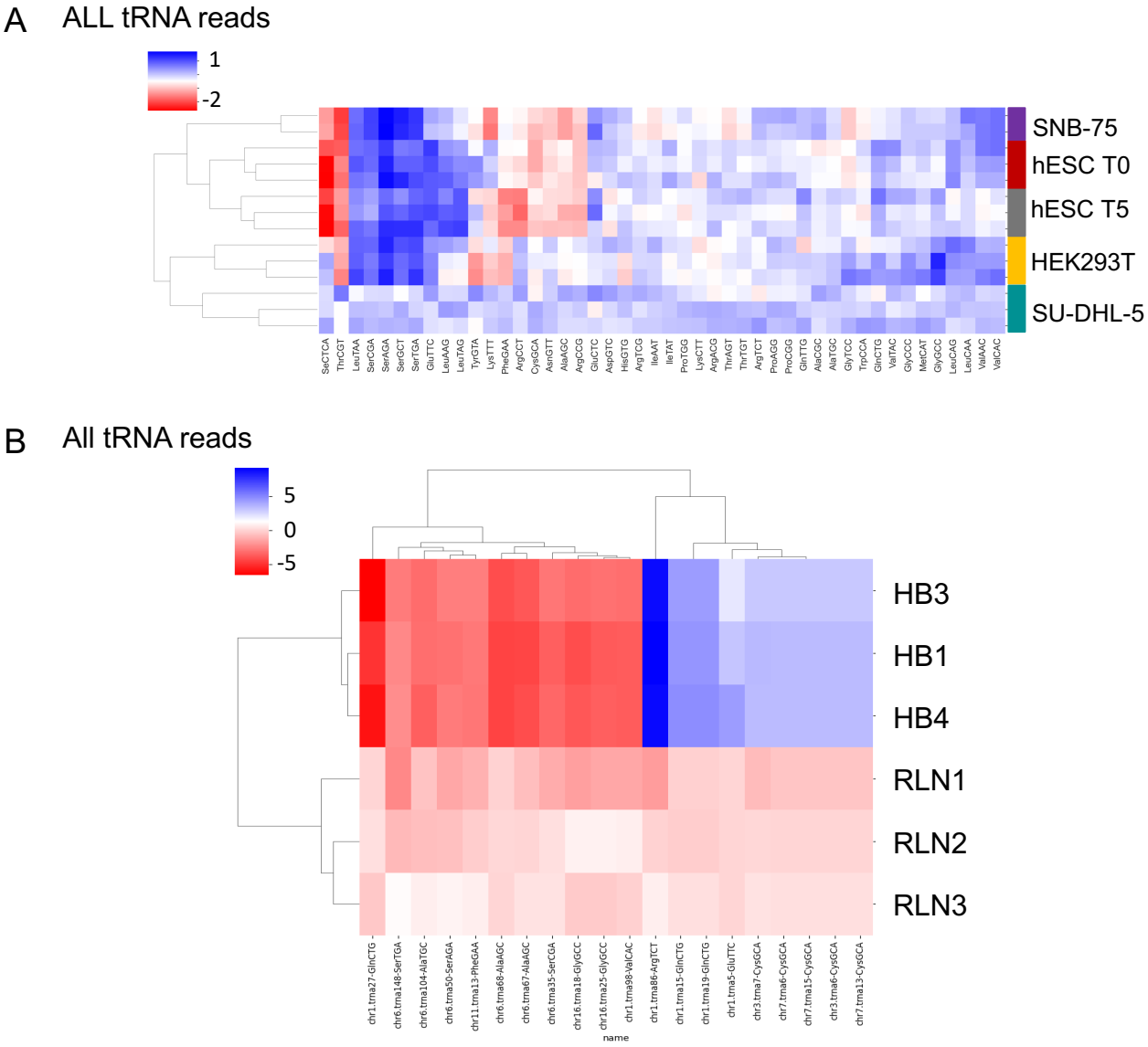

Figure S5. (A) Unsupervised hierarchical clustering of analyzed cell lines. The top two horizontal lines represent SNB-75, followed by triplicates of undifferentiated hESCs at day 0, hESCs 5 days after induction, HEK293T and SU-DHL-5. Expression levels are depicted as (log2) fold change relative to the average of SU-DHL-5. (B) TRNA expression matrix of histologically normal brain (HB) and reactive lymph nodes (RLN). The expression level of the top three horizontal lines represents histologically normal brain and are depicted as (log2) fold change relative to the average of the bottom three lines represented by RLN. (C) Pearson correlation (*r*: 0.35) between RIN values and normalized full-length tRNA reads in 18 GBM samples and 3 normal brain samples of variable RNA quality (RIN values between 4 and 9). (D) Pearson correlation (*r*: -0.78) between normalized rRNA reads below 100 nt and normalized full-length tRNA reads in 18 GBM samples and 3 normal brain samples of variable RNA quality.

Supplemental Figure 6

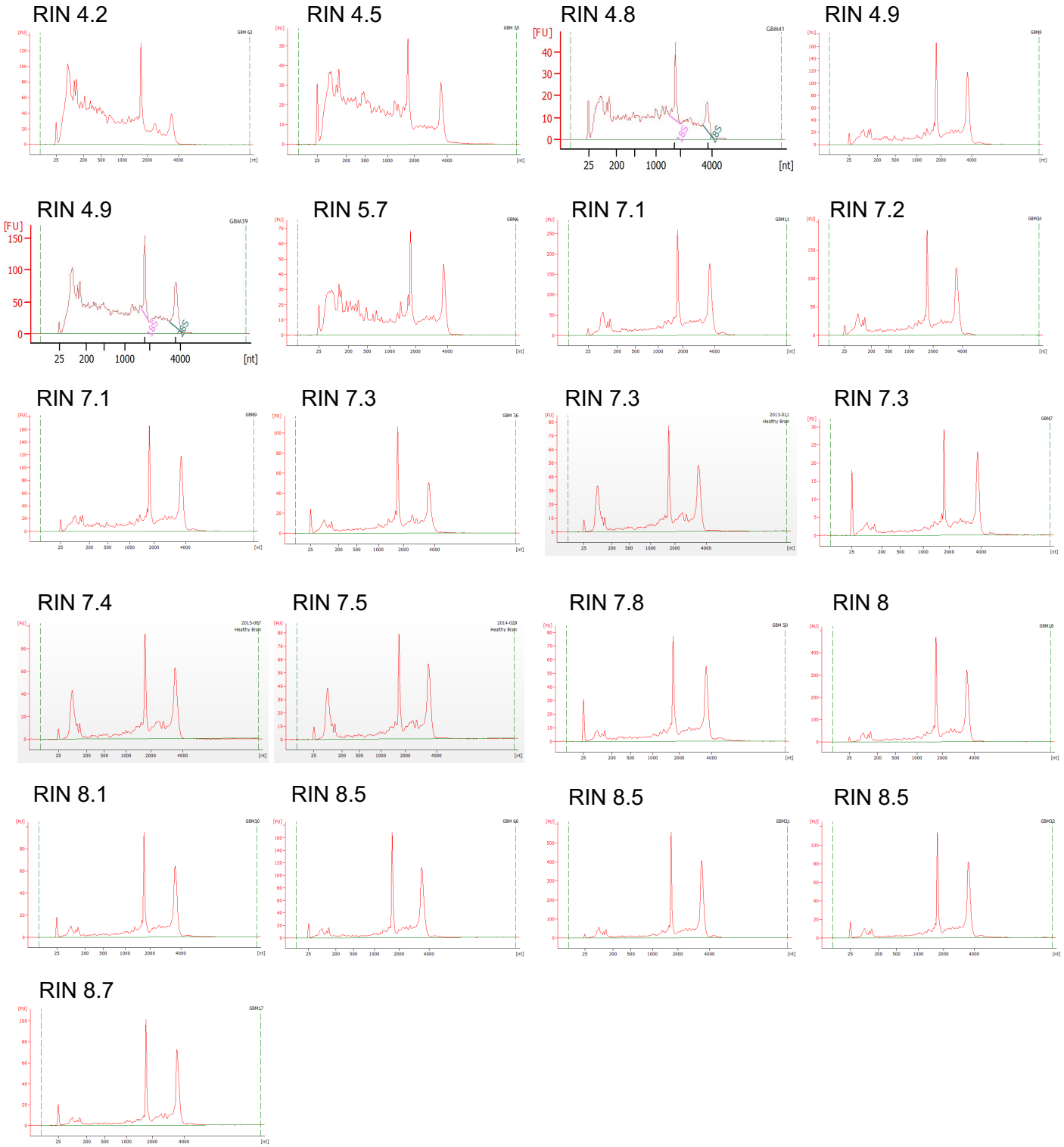

Figure S6. Integrity analysis of total RNA determined by Bioanalyzer. Electropherograms showing 18 GBM and 3 normal brain samples of variable RNA quality. Among 18 tissue samples are 6 sample of low RNA integrity.